# Spectral characterization of dissolved organic matter along trophic gradients: Potential indicators of eutrophication of plateau lakes in Southwest China

**Yuying Guan**
Nanjing Normal University
**Ruiming Han**
Nanjing Normal University
**Nannan Jia**
Institute of Hydrobiology Chinese Academy of Sciences
**Da Huo** ( huoda@ihb.ac.cn )
Institute of Hydrobiology Chinese Academy of Sciences https://orcid.org/0000-0002-3534-1644
**Gongliang Yu**
Institute of Hydrobiology Chinese Academy of Sciences

**Research Article**

**Keywords:** dissolved organic matter, trophic state index, excitation–emission matrix, LASSO

**Posted Date:** June 30th, 2021

**DOI:** https://doi.org/10.21203/rs.3.rs-573085/v1

# Spectral characterization of dissolved organic matter along trophic gradients: Potential indicators of eutrophication of plateau lakes in Southwest China

**Yuying Guan[a,b,1], Ruiming Han[a,c,1], Nannan Jia[b,d], Da Huo[b,d,*], Gongliang Yu[b,*]**

a. School of Environment, Nanjing Normal University, Nanjing 210023, China

b. Key Laboratory of Algal Biology, Institute of Hydrobiology, Chinese Academy of Sciences, Wuhan 430072, People's Republic of China

c. Jiangsu Center for Collaborative Innovation in Geographical Information Resource Development and Application, Nanjing, 210023, China

d. University of Chinese Academy of Sciences, Beijing 100049, People's Republic of China

1 Co-first author

* Corresponding author:

**Author for correspondence:**

Co-corresponding author. Mailing address: Institute of Hydrobiology, Chinese Academy of Sciences, Wuhan 430072, Hubei Province, PR China. Phone: +86 027 68780067. Fax: +86 027 68780123.

Da Huo Email: Huoda@ihb.ac.cn

Gongliang Yu Email: Yugl@ihb.ac.cn

## Declaration

**Ethic approval and consent to participate:** Not applicable

**Consent for publication:** Not applicable

**Availability of data and materials:** Not applicable

**Competing interest: The authors declare that they have no competing interests**

**Funding:** This study was supported by the Scientific Instrument Developing Project of the Chinese Academy of Sciences, Grant No.YJKYYQ20170044, the National Natural Science Foundation of China (41773081, 41703105), the National Water Pollution Control and Treatment Science and Technology Major Project, China (2017ZX07203-003).

**Authors' contributions:** Conceptualization: Yuying Guan, Da Huo; Methodology: Yuying Guan, Da Huo; Formal analysis and investigation: Yuying Guan, Nannan Jia; Writing - original draft preparation: Yuying Guan; Writing - review and editing: Yuying Guan, Ruiming Han; Funding acquisition: Gongliang Yu, Ruiming Han; Resources: Gongliang Yu, Ruiming Han; Supervision: Da Huo, Ruiming Han. All authors read and approved the final manuscript.

**Abstract**

Dissolved organic matter (DOM) acts as a chemical intermediary between terrestrial and lacustrine ecosystems and significantly affects the structure and function of lakes. The optical characteristics of DOM have been widely used to estimate the water quality. However, little is known about its absorption and fluorescence under different trophic states. Especially, comparative research is needed among gradient eutrophic level of plateau lakes when considering their special characteristics. A total of 119 water samples were collected in the Erhai watershed from November 2018 to July 2019 to investigate the optical properties of DOM depending on the trophic state using ultraviolet–visible spectroscopy and parallel factor analysis of the excitation–emission matrix. The water quality conditions in the Erhai watershed were classified using the trophic state index (TSI; 31< TSI < 67). The DOM is largely autochthonous and includes tyrosine-like protein (C1), tryptophan-like protein (C2), and humic-like compounds (C3). Except for an apparent trend of decreasing slope ratio ($S_R$) ($p < 0.01$), both absorption coefficient at 254 nm and fluorescence intensity increase with the rising trophic state ($p < 0.01$). In this study, new models ($R^2_{aCDOM(254)} = 0.762$; $R^2_{Fn(355)} = 0.705, p < 0.01$) basing on significant correlations between the TSI and $a_{CDOM}(254)$ and Fn(355) were established to predict the trophic state. The results of this study demonstrate that the effects of nutrients and environmental factors (pH and water temperature) on DOM vary depending on the trophic state and that the pH plays the main role in DOM production. Our analyses highlight the importance of DOM in aquatic ecosystems and the correlation between TSI and the optical properties of DOM. Our research unmasks the strong linkage between optical parameters of DOM and freshwater quality by applying neural network prediction.

**Keywords:** dissolved organic matter, trophic state index, excitation–emission matrix, LASSO

# 1. Introduction

Because of the continuous increase in the population and the rapid advancement of industrialization and agricultural modernization in China, many nutrients are discharged into lakes along with sewage, resulting in increased nitrogen and phosphorus concentrations in lakes and eutrophication, which is problematic (Smith 2003). Eutrophication is defined as the increase in the productivity of phytoplankton and aquatic plants and deterioration of the water due to the increasing nutrient concentration of the water (James et al. 2005, Tang et al. 2010). It is accompanied by bloom occurrences and declining aquatic plant species richness and ecosystem functions (Tang et al. 2010). The increase in the phytoplankton biomass in eutrophic lakes leads to an increase in the number of organic aggregates and thus the number of adhesive bacteria and decreases the concentration of dissolved oxygen. This process is called anoxia-driven "vicious cycle" (Meinhard et al. 2002, Smith and Schindler 2009). Thus, it is necessary to evaluate the eutrophic status of lakes.

Vollenweider (1968) classified the trophic state of lakes using the nitrogen and phosphorus concentrations and proposed a five-level classification system. However, because his classification system relies only on nitrogen and phosphorus, its application is limited. In general, phytoplankton, which reflects the primary productivity of aquatic systems, plays an important role in eutrophication. The Organization for Economic Co-operation and Development (OECD) established a new classification system using chlorophyll a (Chl-a), the Secchi disk depth (SDD), and the total phosphorus (TP) concentration (OECD 1982). Carlson presented a modified approach to improve the sensitivity of the traditional classification (Carlson 1977). These classification systems were derived from laboratory indicators that are susceptible to environmental factors; as a result, the assessment of the trophic state is susceptible to interferences. Therefore, a new method must be

85 developed to predict the trophic state using parameters that can be obtained at high temporal and
86 spatial resolutions.

87 Dissolved organic matter (DOM) is a typical dissolved organic mixture with a complex
88 composition, which affects the structure and function of water ecosystems in association with the
89 eutrophication of waterbodies (Mackay et al. 2020). It has been suggested that primarily
90 allochthonous DOM, which originates from anthropogenic activities and is then transferred via
91 terrestrial and river imports into lakes, leads to eutrophication (Hudson et al. 2010, Shang et al.
92 2018). The generation and transformation of DOM can affect the nutrient cycle in aquatic
93 environments; the photosynthesis of phytoplankton is one of the major sources of DOM (Malkin et
94 al. 2008, Mostofa and Sakugawa 2009). The correlation between the spectral characteristics of DOM
95 and eutrophication has received widespread attention (Liu et al. 2020, Zhao et al. 2019, Zhou et al.
96 2018). Based on ultraviolet–visible (UV–Vis) spectroscopy and excitation–emission matrix
97 spectroscopy coupled with parallel factor analysis (EEM-PARAFAC), the DOM source and
98 composition vary depending on the trophic state (Birdwell and Engel 2010, Wang et al. 2019, Yao
99 et al. 2011). Although the mechanism linking DOM with eutrophication remains unclear, their
100 correlation provides new insights into the eutrophication process of lakes, differing from the
101 traditional evaluation using total nitrogen, total phosphorus, and other inorganic salts (Shang et al.
102 2018). The trophic state can be defined by the nutrient-color paradigm including the optical
103 parameters of colored DOM (CDOM) and fluorescent DOM (FDOM; (Effler et al. 2010, Weishaar
104 et al. 2003, Zhang et al. 2010, Zhao et al. 2016). For example, $a_{CDOM}(254)$ and the humification
105 index (HIX) have been used to establish a new eutrophic classification based on 22 lakes (Zhang et
106 al. 2018) and 131 reservoirs across China (Shang et al. 2019b). In both models, the correlation

between the absorption or fluorescent characteristics of DOM and the trophic state index (TSI) has been considered. However, the optical properties of DOM differ in different regions. Regional DOM characteristics in various aquatic environments affected by different physicochemical parameters remain unclear (Findlay and Sinsabaugh 2004).

Because DOM is closely linked to nutrients, several researchers have focused on studying eutrophic lakes in the Yangtze River (Zhang et al. 2005, Zhang et al. 2007). Compared with plain lakes, the unique climate and long water exchange period of plateau lakes contribute to a more fragile ecosystem and altered DOM optical properties. However, there is a lack of research on the optical properties (absorption and fluorescence) of DOM and the correlations between DOM and environmental factors for plateau lakes. The Erhai watershed, including Lake Cibi, Lake Xihu, Lake Erhai, and other branches in the Yunnan–Guizhou Plateau, is representative of the steady-state conversion of grass and algae. In recent years, the organic matter and phytoplankton biomass increased in the Erhai watershed and cyanobacterial blooms are common, threatening aquatic ecosystems and human health (Jiang et al. 2013). However, the correlations between the optical properties of DOM and the water quality under various trophic states of typical plateau lakes have not been determined.

Therefore, the main aims of this study were to determine: (1) the optical properties of DOM under various trophic states, (2) relationship between the DOM properties and TSI, and (3) environmental factors that influence DOM under diverse trophic states.

## 2. Materials and methods

## 2.1 Study area

The Erhai watershed is located in the Dali Prefecture, Yunnan Province, China, and includes Lake Erhai (EH), Lake Cibi (CBH), Lake Xihu (XH) as well as the Luoshi, Yongan, Luoshi, and Miju rivers. Lake Erhai is the main lake of this watershed and the second largest one in southwestern China, with a surface area of 249.8 $km^2$ and an average water depth of 10.5 m. Its water mainly originates from precipitation and snowmelt. Among the 117 rivers entering the lake, the main rivers are Miju and Luoshi in the north and the Cangshan Eighteen Stream in the west. The rivers in the northern part account for 70% of the annual inflow to Lake Erhai. Lake Cibi and Lake Xihu have small surface areas and are in the upper reaches of Lake Erhai with concentrated agricultural development. The domestic pollution and tourism development in the western part of Lake Erhai are significant. The region is affected by monsoon climate, with dry (November to April of the following year) and wet (May to October, 95% of the precipitation) seasons.

## 2.2 Field sampling and sample collection

Four field campaigns were carried out in November 2018 and January, April, and July 2019. All field campaigns were conducted in clear weather conditions, except for that in July. In total, 119 water samples were collected (Fig. 1). Surface water samples (0.5 m) were collected using clean polyethylene bags and immediately shipped back to the laboratory for further analysis. All samples were divided into two categories. A portion of the samples was filtered using a Whatman GF/C filter and the water quality parameters were analyzed. In preparation for the spectral analyses of CDOM and FDOM, several samples were filtered using a precombusted (450 °C, 3 h) Whatman GF/F filter and 0.2 μm Millipore filter and filled into 150 mL acid-washed amber glass bottles.

## 2.3 Optical measurements and analysis

Absorption spectra of CDOM were measured using a UV-2550 UV–Vis spectrophotometer (Shimadzu, Japan). The absorption coefficients of CDOM were obtained using the following equation (Bricaud and Prieur 1981):

$$a_{CDOM}(\lambda) = 2.303 \times \frac{OD(\lambda)}{L} \qquad (1)$$

where $a_{CDOM}(\lambda)$ is the CDOM absorption coefficient at a given wavelength ($\lambda$), $OD(\lambda)$ is the corrected optical density at wavelength $\lambda$, and L is the cuvette path length (0.1 m). To eliminate the effects of internal backscattering, the absorbance at 700 nm was used for the correction of the absorption coefficient (Song et al. 2012). The absorption spectra of the filtered water samples were measured between 200 and 800 nm at 1 nm intervals. Milli-Q water was used as a reference. Because of the chemical complexity of CDOM, the concentration of CDOM was expressed using the absorption coefficient at 254 nm (Song et al. 2019, Wei et al. 2019).

The spectral slopes ($S$) between 275 and 295 nm ($S_{275–295}$) and between 350 and 400 nm ($S_{350–400}$) were calculated using least squares fitting (Song et al. 2019). The slope $S_{275-295}$ reflects the composition, molecular weight, and photochemical reactivity of the DOM (Helms et al. 2008, Xiao et al. 2013). The $S_{275–295}/S_{350–400}$ ratio ($S_R$) was used as a proxy for the molecular weight of the DOM, which is related to its source and composition (Helms et al. 2008). The parameter $SUVA_{254}$ is the absorbance at 254 nm divided by the DOC concentration (Weishaar et al. 2003). The parameter M is the ratio of the absorption coefficient at 250 nm to that at 365 nm and reflects the molecular weight (Helms et al. 2008, Peuravuori and Pihlaja 1997).

Fluorescence EEM spectroscopy was performed using a Cary Eclipse fluorescence

169 spectrometer (Agilent, Malaysia) with a maximum emission intensity of 1000 arbitrary units (AU;
170 (Sha et al. 2019). The excitation (Ex) and emission (Em) slits were both 5 nm. The excitation
171 wavelength was set to 210–450 nm (5 nm intervals). The emission wavelength was set to 250 to 600
172 nm and the fluorescence spectrum was obtained at intervals of 1 nm. Data obtained with
173 fluorescence EEM spectroscopy were used for PARAFAC using the *N*-way toolbox of MATLAB
174 2014a and parafacmodelingV2.0 package (Andersson and Bro 2000) (Razavi et al. 2021). The three-
175 dimensional fluorescence spectrum of Milli-Q water was subtracted from the measured spectra to
176 correct for the Raman scattering of water (Shang et al. 2019a, Wei et al. 2019). A 290 nm cutoff was
177 used for all samples to limit the second-order Rayleigh scattering (Sha et al. 2019, Zhang et al. 2016).
178 Quinine sulfate (QS) solution (1 μg of QS $L^{-1}$ in 0.1 M $H_2SO_4$) was used to monitor the stability of
179 the energy emitted by the xenon lamp. The number of individual components was determined using
180 split-half and load analyses.

181 The biogenic index (BIX) is the ratio of the emission wavelength (380–430 nm) to the
182 excitation wavelength of 310 nm (Huguet et al. 2009, Wickland et al. 2007). The fluorescence index
183 (FI) is the ratio of the emission wavelength (470–520 nm) to the excitation wavelength (370 nm;
184 (Cory and Mcknight 2005). The Fn(355) is the intensity of the emission spectrum at $\lambda_{EM}$ = 450 nm
185 after excitation with a wavelength of $\lambda_{EX}$ = 355 nm and indicates the relative concentration of humic-
186 like compounds (Chen et al. 2012). For the comparison with other indicators, Fn(355) was reported
187 on a logarithmic scale.

188 ## 2.4 Other parameters

189 The DOC was analyzed by high-temperature catalytic oxidation using a TOC-L Analyzer

(Shimadzu, Japan). Water quality parameters refer to the Environmental Quality Standards for Surface Water (GB383-2002, China). The Chl-a was obtained by extraction with 90% alcohol.

The TSI was calculated using the following four equations (Wei et al. 2019):

$$TSI = 0.421 * TSI\ (Chl\text{-}a) + 0.282 * TSI\ (TN) + 0.297 * TSI\ (TP) \quad (2)$$

$$TSI\ (Chl\text{-}a) = 10 * (2.5 + 1.086 * \ln Chl\text{-}a) \quad (3)$$

$$TSI\ (TN) = 10 * (5.453 + 1.694 * \ln TN) \quad (4)$$

$$TSI\ (TP) = 10 * (9.436 + 1.624 * \ln TP) \quad (5)$$

$30 \leqslant TSI < 50$, $50 \leqslant TSI < 60$, $60 \leqslant TSI < 70$, and $TSI > 70$ indicates mesotrophic, lightly eutrophic, moderately eutrophic, and hypereutrophic conditions, respectively.

## 2.5 Statistical analysis

The mean values and standard deviations are reported, which were calculated using EXCEL 2013 software. The software RStudio was used for linearity or nonlinearity and Kruskal–Wallis (K–W) tests; the disparity was considered significant when $p < 0.05$. The data were plotted using RStudio and the ggplot2 package. Spatial mapping of the sampling sites was conducted using ArcGIS 10.3. Least absolute shrinkage and selection operator (LASSO) analysis was employed to identify the potential drivers of the DOM properties and resolve variable collinearity problems. The data were normalized using the maximum and minimum methods. Principal component analysis (PCA) was used to identify important environmental factors. The neural network was used to estimate the TSI and the coefficient of determination ($R^2$) and root-mean-square error (RMSE) between the measured and predicted TSIs were calculated to assess the validation accuracy. The RMSE was determined using Eq. (6).

$$RMSE=\sqrt{\frac{1}{n}\times\sum_{1}^{n}[Mea.TSI - Pre.TSI]^2}, \quad (6)$$

where Mea,TSI is the measured TSI and Pre.TSI is the TSI predicted using the neural network model.

# 3. Results

## 3.1 Water quality characteristics

All samples from the Erhai watershed (CBH, XH, EH, and rivers) were divided into mesotrophic, light-eutrophic, and middle-eutrophic ($30 < TSI < 67$) categories. The concentrations of TN, TP, Chl-a, $NH_4^+$-N, $NO_3^-$-N, and DOC in the samples from the study area were determined (Table 1). The DOC concentration ranges from 1.9 to 11.13 mg $L^{-1}$. The highest mean value (7.30 ± 2.70 mg $L^{-1}$) was obtained for the middle-eutrophic samples. The TN concentrations of the mesotrophic samples are lower than those of the light- and middle-eutrophic samples. The TP concentrations range from 0.01 to 0.25 mg $L^{-1}$. The TP concentration of moderately eutrophic water is higher than that of other water. The average Chl-a concentration ranges from 1.39-119.74 μg $L^{-1}$. The average $NH_4^+$-N and $NO_3^-$-N concentrations significantly vary, ranging from 0.002 to 0.27 mg $L^{-1}$ and from 0.004 to 2.20 mg $L^{-1}$, respectively. The samples used in this study were classified as mesotrophic (n = 65), lightly eutrophic (n = 38), and moderately eutrophic (n = 16).

## 3.2 DOM absorption characteristics

A significant difference was observed for $a_{CDOM}(254)$ for the wet–dry season depending on the trophic state ($p < 0.01$; Fig.2). The $a_{CDOM}(254)$ of all samples ranges from 5.74 to 67.50 $m^{-1}$. The mean $a_{CDOM}(254)$ value of middle-eutrophic samples (24.92 ± 14.02 $m^{-1}$) is notably higher than that of mesotrophic (16.06 ± 8.08 $m^{-1}$) and light-eutrophic samples (20.24 ± 8.64 $m^{-1}$). The M value ranges from 2.32 to 10.72 throughout the year. In the dry season, M and $S_R$ significantly differ ($p <$

232 0.05). The values of the middle-eutrophic samples obtained in the dry season are lower than those
233 of the light-eutrophic and mesotrophic samples (Fig. 2b). The $S_R$ values range from 0.88 to 1.24;
234 most samples exhibit values above 1. The $S_{275–295}$ values obtained for the wet–dry season
235 insignificantly differ among different trophic states (Fig. 2). The SUVA254 value varies in the wet
236 season but not in the dry season. In the wet season, the highest value (2.33 ± 0.61) was obtained for
237 light-eutrophic samples, followed by mesotrophic samples.

238 ## 3.3 DOM fluorescence characteristics

239 Based on EEM analysis, three fluorescence components were identified (Table S1). The
240 relative distribution of individual components differs depending on the trophic state (Fig. S1). The
241 first component (C1) peaks at $\lambda_{EX/EM}$ = 220/292 nm and was determined to be a tyrosine-like protein
242 (Fig. 3) (Chen et al. 2003). The second component (C2) has an intense peak at $\lambda_{EX}$ = 230 nm and
243 $\lambda_{EM}$ = 356 nm and was determined to be a tryptophan-like protein, which is commonly related to the
244 fluorescent group of aromatic protein structures produced by microbial degradation (Chen et al.
245 2003, Cory and Kaplan 2012, Stedmon and Markager 2005). The third component (C3) shows one
246 peak ($\lambda_{EX}$ = 245 nm, $\lambda_{EM}$ = 458 nm) with excitation and emission characteristics similar to humic-
247 like DOM that formed from soil or plants during terrestrial or autochthonous phytoplankton
248 degradation or bacterial activity (Fellman et al. 2011, Wei et al. 2019, Zhang et al. 2009).

249 The range of Fn(355) values varies from 1.16 to 2.97. The average Fn(355) value increases
250 from mesotrophic samples (1.92 ± 0.31) to light-eutrophic samples (2.06 ± 0.29) to middle-
251 eutrophic samples (2.24 ± 0.19; Fig. S1). In contrast to the dry season, the FI of all samples does
252 not differ in the wet season (Fig. 2). In dry-season samples, the FI values are the highest in light-
253 eutrophic samples (3.43 ± 1.94). The different BIX values obtained for the dry season and various

trophic states are statistically significant ($p < 0.01$; Fig. 2b). The BIX of all samples ranges from 0.72 to 3.16, with an average of 1.39 ± 0.67 for light-eutrophic samples, 1.22 ± 0.58 for mesotrophic samples, and 1.02 ± 0.50 for middle-eutrophic samples. The FI is higher than 1.9 in 96 of the 119 samples and BIX is higher than 0.8 in 109 of the 119 samples, indicating that the DOM in Lake Erhai is predominantly derived from autochthonous sources.

## 3.4 Correlation between DOM properties and trophic state

There were no significant correlations between $S_R$, $SUVA_{254}$, $S_{275\text{-}295}$, M, and TSI ($R = -0.29$, $R = 0.14$, $R = -0.06$, $R = -0.19$, $p < 0.05$; Fig. 4). The significant positive correlations between TSI and $a_{CDOM}(254)$ and Fn(355) ($R = 0.56$, $R = 0.41$, $p < 0.05$) indicate that $a_{CDOM}(254)$ and Fn(355) can be used as indicators of the trophic state in the Erhai watershed (Fig. 4). Sixty-four water samples were used to calibrate the model and the remaining samples were used for the validation. The results of the validation of the predicted model are presented in Fig. 5. The adjusted coefficients of determination of $a_{CDOM}(254)$ and Fn(355) are 0.76 and 0.71, with RMSE values of 3.40 and 4.20, respectively. The BIX is positively correlated with the trophic state ($R = -0.30$, $p < 0.05$) and there is no significant correlation between TSI and FI ($R = 0.12$, $p > 0.05$). Overall, $a_{CDOM}(254)$ and Fn(355) significantly correlate with TSI and thus can be used to assess the trophic state in the Erhai watershed.

To determine why the composition of DOM in various trophic states differs, the correlations between environmental variables (pH, temperature, TN, TP, $NH_4^+$-N, $NO_3^-$-N, and Chl-a) and FDOM [Fn(355)] were analyzed using the LASSO model (Fig. 4). The results show that the pH, TN, and $NO_3^-$-N significantly correlate with FDOM in mesotrophic samples. In light-eutrophic waters, the pH, TP, $NH_4^+$-N, and Chl-a significantly correlate with the fluorescence of the DOM. In

middle-eutrophic samples, significant correlations between the pH, water temperature, TN, and FDOM were observed. Regardless of the trophic state, the pH affects the FDOM, whereas the effects of most other variables differ depending on the trophic state.

# 4. Discussion

## 4.1 Optical characteristics of DOM depending on the trophic state

The $a_{CDOM}(254)$ and TSI ($R = 0.36$, $R = 0.56$, $p < 0.05$) are positively correlated, indicating that eutrophication increases the DOM concentration by promoting phytoplankton growth and organic matter accumulation (Song et al. 2018). A possible explanation may be that the rate of photosynthesis in eutrophic samples is always greater than that in oligotrophic and mesotrophic samples (Pacheco et al. 2014, Ye et al. 2015). The CDOM absorption values obtained for the study area are lower than those reported for freshwater lakes in China (average of 19.55; (Song et al. 2019). The M values obtained for middle-eutrophic samples are lower than those of mesotrophic samples (Fig. 2). This result is similar to that of Brandão et al. (2016) who reported that the M value of hypereutrophic reservoirs is lower than that of oligotrophic lakes.

Our results show that the fluorescence components in the Erhai watershed are dominated by humic-like components (C3; Fig. S1), which differs from several other cases in which autochthonous protein-like components play the main role such as in lakes of the Yungui Plateau and other plateaus (Hood et al. 2003, Miller et al. 2009, Zhang et al. 2009). This difference may be due to the complex geographical and hydrological conditions and other environmental factors. The results of a previous study showed that an increase in the phytoplankton biomass contributes to an increase of humic-like components in nutrient-rich water samples (Miller et al. 2009). The FDOM

297 values of lakes and rivers in the middle-eutrophic state are higher than those in the mesotrophic state
298 (Fig. S1). These results are similar to those reported for lakes in the Yungui Plateau. Zhang et al.
299 (2010) suggested that an increase in the trophic state of the lakes in the Yungui Plateau leads to an
300 increase of humic-like components due to the increased degradation of terrestrial nutrients and
301 phytoplankton biomass. The results of several previous studies are consistent with this hypothesis
302 (Miller et al. 2009, Zhang et al. 2009).

303 Based on the previously reported results, several indicators can be used to explain the change
304 in the source of DOM. It has been demonstrated that the FI is a key indicator of the DOM source.
305 Lower FI values (~1.4) indicate terrestrial sources and higher FI values (~1.9) indicate
306 autochthonous sources (Mcknight et al. 2001, Wolfe et al. 2002). Based on the positive correlation
307 between FI and humic-like components (C3; $R = 0.32$, $p < 0.05$) observed in our study and the high
308 FI of the samples (>1.9), the DOM is autochthonous and was produced by biota in the aquatic
309 ecosystem (Traving et al.). The value of BIX ranges from 0.72 to 3.16, representing biological or
310 aquatic bacteria-dominated DOM (Huguet et al. 2010, Parlanti et al. 2000). This indicates an intense
311 microbial activity at most sampling sites. However, data related to microorganisms were not
312 obtained in this study. Therefore, the contribution of microbial activity to DOM must be analyzed
313 and discussed in future studies.

314 ## 4.2 Effects of $a_{CDOM}(254)$ and Fn(355) on TSI

315 Many researchers have focused on the classification of the trophic states in aquatic ecosystems
316 and mostly utilized inorganic nutrient concentrations and phytoplankton (Carlson 1977, Cunha et al.
317 2013). Considering the correlations between the optical properties of DOM and the trophic states,
318 it has been proposed that the trophic state can be identified using CDOM absorption (Webster et al.

2008, Zhang et al. 2018). The HIX has been used to define the trophic state of reservoirs (Shang et al. 2019b). Based on the results of PCA, the samples in Lake Erhai were classified into four groups (CBH, EH, R, and XH) with notable geographical features (Fig. S2). Our results show that different lakes can be distinguished based on the optical parameters of DOM under various trophic states. The significant correlations between $a_{CDOM}(254)$ and Fn(355) and the TSI indicate that the eutrophication intensifies with increasing DOM concentration (Figs 4 and 5).

Previous studies showed that the trophic state depends on the input of nutrients and organic matter (Kissman et al. 2017). Based on the significant correlations between the trophic state and $a_{CDOM}(254)$ and Fn(355) in the Erhai watershed, we propose a new approach to determine the trophic state of plateau lakes utilizing the absorption and fluorescence characteristics of DOM. Shortcomings of traditional methods can be avoided by predicting eutrophication based on the optical parameters of DOM, especially the CDOM absorption coefficient. As one of the important parameters of water color remote sensing, CDOM can be used for large-scale eutrophication monitoring. The new models established in our study include water samples from various trophic states and thus are applicable to other plateau lakes. However, uncertainties are likely when the models are applied to oligotrophic and hypereutrophic samples. Therefore, more data from other lakes and rivers must be obtained to improve the applicability of the new models.

### 4.3 Factors affecting DOM in various trophic states

The strong positive correlations between the optical properties of DOM and TSI indicate that DOM is affected by variations in nutrients. The results of a previous study of the Inner Mongolia Plateau support this correlation (Wen et al. 2016). Variables obtained from the LASSO model suggest that the effects of nutrient and environmental factors on DOM (expressed by FDOM) differ

depending on the trophic state. The pH correlates with FDOM, independent of the trophic state. The highest pH value was observed under light-eutrophic conditions. The results of previous studies showed that the pH has a significant effect on the photolysis rate and absorbance of DOM (Timko et al. 2015). In mesotrophic samples, the pH, $NO_3^-$-N, and TN may affect FDOM; $NO_3^-$-N seemingly plays a dominant role. The concentration of $NO_3^-$-N is relatively high in mesotrophic samples and thus more protein can be synthesized by metabolic reduction, leading to the highest proportion of protein (48%) in mesotrophic water. The high $NO_3^-$-N content increases the nutrient availability, promotes $CO_2$ production, and enhances microbial activity in ecosystems, thereby increasing the proportion of autochthonous DOM (Bridgham and Richardson 2003, Treseder 2008). With increasing nutrient levels, the importance of the pH decreases and the effects of the $NH_4^+$-N concentration are enhanced. In the light-eutrophic state, the concentrations of $NH_4^+$-N in rivers are higher, leading to higher FDOM concentrations. This may be due to high levels of inorganic N, which stimulate phytoplankton production (Hounshell et al. 2017). The results of previous studies showed that TP and Chl-a are key factors in determining the degree of humification and that the pH generally increases the P availability (Moore Jr and Reddy 1994, Zhi et al. 2015). Because of the intensification of eutrophication, TN has the greatest effect on the FDOM concentration. This might be due to the nitrogen and phosphorus availabilities, which lead to seasonal differences in the DOM properties but also affect the DOM release by phytoplankton and heterotrophic degradation by bacteria (Asmala et al. 2018). The middle-eutrophic samples mostly originate from Lake Xihu, which is severely affected by human activities and thus an elevated nutrient input, resulting in an increase in the DOM concentration due to microbial activity (Williams et al. 2016).

# 5. Conclusions

In this study, the characteristics of CDOM absorption and DOM fluorescence in the Erhai watershed in the Yunnan Province, China, were analyzed. Compared with mesotrophic samples, middle-eutrophic samples exhibit higher absorption coefficients and fluorescence intensities. Three fluorescence components were identified by the PARAFAC model: tyrosine-like (C1), tryptophan-like (C2), and humic-like (C3) components. The results of the fluorescence and absorption analyses indicate the low molecular weight and autochthonous sources of DOM. Based on their strong correlation, $a_{CDOM}(254)$ and Fn(355) can be used as indicators of the trophic state of plateau lakes. The factors affecting FDOM depend on the trophic state. However, the pH is the main environmental factor influencing the production of DOM regardless of the trophic state, followed by the nitrogen and phosphorus concentrations. The correlations between the DOM properties and trophic states highlighted in this study can be used for the rapid monitoring of the water quality.

# Reference


Andersson, C.A. and Bro, R. (2000) The N-way Toolbox for MATLAB. Chemometrics and Intelligent Laboratory Systems 52(1), 1-4.

Asmala, E., Haraguchi, L., Jakobsen, H.H., Massicotte, P. and Carstensen, J. (2018) Nutrient availability as major driver of phytoplankton-derived dissolved organic matter transformation in coastal environment. Biogeochemistry 137(1), 93-104.

Birdwell, J.E. and Engel, A.S. (2010) Characterization of dissolved organic matter in cave and spring waters using UV–Vis absorbance and fluorescence spectroscopy. Organic Geochemistry 41(3), 270-280.

Brandão, L.P.M., Staehr, P.A. and Bezerra-Neto, J.F. (2016) Seasonal changes in optical properties of two contrasting tropical freshwater systems. Journal of Limnology 75(3), 508-519.

Bricaud, A. and Prieur, M.L. (1981) Absorption by Dissolved Organic Matter of the Sea (Yellow Substance) in the UV and Visible Domains. Limnology & Oceanography 26(1), 43-53.

Bridgham, S.D. and Richardson, C.J. (2003) Endogenous versus exogenous nutrient control over decomposition and mineralization in North Carolina peatlands. Biogeochemistry 65(2), 151-178.

Carlson, R. (1977) A Trophic State Index for Lakes. Limnology and Oceanography - LIMNOL OCEANOGR 22, 361-369.

Chen, W., Westerhoff, P., Leenheer, J.A. and Booksh, K. (2003) Fluorescence Excitation−Emission Matrix Regional Integration to Quantify Spectra for Dissolved Organic Matter. Environmental Science & Technology.

Chen, X., Chuai, X., Yang, L. and Zhao, H. (2012) Climatic warming and overgrazing induced the high concentration of organic matter in Lake Hulun, a large shallow eutrophic steppe lake in northern China. Science of The Total Environment 431, 332-338.

Cory, R.M. and Kaplan, L.A. (2012) Biological lability of streamwater fluorescent dissolved organic matter. Limnology and Oceanography 57(5), 1347-1360.

Cory, R.M. and Mcknight, D.M. (2005) Fluorescence spectroscopy reveals ubiquitous presence of oxidized and reduced quinones in dissolved organic matter. Environmental Science & Technology 39(21), 8142-8149.

Cunha, D.G.F., Calijuri, M.d.C. and Lamparelli, M.C. (2013) A trophic state index for tropical/subtropical reservoirs (TSItsr). Ecological Engineering 60, 126-134.

Effler, S.W., Perkins, M., Peng, F., Strait, C., Weidemann, A.D. and Auer, M.T. (2010) Light-absorbing components in Lake Superior. Journal of Great Lakes Research 36(4), 656-665.

Fellman, J.B., Petrone, K.C. and Grierson, P.F. (2011) Source, biogeochemical cycling, and fluorescence characteristics of dissolved organic matter in an agro-urban estuary. Limnology and Oceanography 56(1), 243-256.

Findlay, S.E.G. and Sinsabaugh, R.L. (2004) Aquatic ecosystems: interactivity of dissolved organic matter. Journal of the North American Benthological Society 23(3), 662-663.

Helms, J.R., Stubbins, A., Ritchie, J.D., Minor, E.C., Kieber, D.J. and Mopper, K. (2008) Absorption spectral slopes and slope ratios as indicators of molecular weight, source, and photobleaching of chromophoric dissolved organic matter. Limnology and Oceanography 53(3), 955-969.

Hood, E., McKnight, D.M. and Williams, M.W. (2003) Sources and chemical character of dissolved organic carbon across an alpine/subalpine ecotone, Green Lakes Valley, Colorado Front Range,

United States. Water Resources Research 39(7).
Hounshell, A.G., Peierls, B.L., Osburn, C.L. and Paerl, H.W. (2017) Stimulation of Phytoplankton Production by Anthropogenic Dissolved Organic Nitrogen in a Coastal Plain Estuary. Environmental Science & Technology 51(22), 13104-13112.
Hudson, N., Baker, A. and Reynolds, D. (2010) Fluorescence analysis of dissolved organic matter in natural, waste and polluted waters—a review. River Research & Applications 23(6), 631-649.
Huguet, A., Vacher, L., Relexans, S., Saubusse, S., Froidefond, J.M. and Parlanti, E. (2009) Properties of fluorescent dissolved organic matter in the Gironde Estuary. Organic Geochemistry 40(6), 706-719.
Huguet, A., Vacher, L., Saubusse, S., Etcheber, H., Abril, G., Relexans, S., Ibalot, F. and Parlanti, E. (2010) New insights into the size distribution of fluorescent dissolved organic matter in estuarine waters. Organic Geochemistry 41(6), 595-610.
James, C., Fisher, J., Russell, V., Collings, S. and Moss, B. (2005) Nitrate availability and hydrophyte species richness in shallow lakes. Freshwater Biology 50(6), 1049-1063.
Jiang, Y., Yu, G., Chai, W., Song, G. and Li, R. (2013) Congruence between mcy based genetic type and microcystin composition within the populations of toxic Microcystis in a plateau lake, China. Environmental Microbiology Reports 5(5), 637-647.
Kissman, C.E.H., Williamson, C.E., Rose, K.C. and Saros, J.E. (2017) Nutrients associated with terrestrial dissolved organic matter drive changes in zooplankton:phytoplankton biomass ratios in an alpine lake. Freshwater Biology 62(1), 40-51.
Liu, D., Du, Y.X., Yu, S.J., Luo, J.H. and Duan, H.T. (2020) Human activities determine quantity and composition of dissolved organic matter in lakes along the Yangtze River. Water Research 168, 11.
Mackay, E.B., Feuchtmayr, H., De Ville, M.M., Thackeray, S.J., Callaghan, N., Marshall, M., Rhodes, G., Yates, C.A., Johnes, P.J. and Moberly, S.C. (2020) Dissolved organic nutrient uptake by riverine phytoplankton varies along a gradient of nutrient enrichment. Science of the Total Environment 722, 14.
Malkin, S.Y., Guildford, S.J. and Hecky, R.E. (2008) Modeling the growth response of Cladophora in a Laurentian Great Lake to the exotic invader Dreissena and to lake warming. Limnology and Oceanography 53(3), 1111-1124.
Mcknight, D.M., Boyer, E.W., Westerhoff, P.K., Doran, P.T., Kulbe, T. and Andersen, D.T. (2001) Spectrofluorometric Characterization of Dissolved Organic Matter for Indication of Precursor Organic Material and Aromaticity. Limnology & Oceanography 46(1), 38-48.
Meinhard, S., Hans-Peter, G., Bernd, S. and Helle, P. (2002) Microbial ecology of organic aggregates in aquatic ecosystems. Aquatic Microbial Ecology 28(2), 175-211.
Miller, M.P., McKnight, D.M., Chapra, S.C. and Williams, M.W. (2009) A model of degradation and production of three pools of dissolved organic matter in an alpine lake. Limnology and Oceanography 54(6), 2213-2227.
Moore Jr, A. and Reddy, K.R. (1994) Role of Eh and pH on Phosphorus Geochemistry in Sediments of Lake Okeechobee, Florida. Journal of Environmental Quality 23(5), 955-964.
Mostofa, K.M.G. and Sakugawa, H. (2009) Spatial and temporal variations and factors controlling the concentrations of hydrogen peroxide and organic peroxides in rivers. Environmental Chemistry 6(6), 524-534.

OECD (1982) Eutrophication of Water Monitoring. Assessment & Control.
Pacheco, F.S., Roland, F. and Downing, J.A. (2014) Eutrophication reverses whole-lake carbon budgets. Inland Waters 4(1), 41-48.
Parlanti, E., Wörz, K., Geoffroy, L. and Lamotte, M. (2000) Dissolved organic matter fluorescence spectroscopy as a tool to estimate biological activity in a coastal zone submitted to anthropogenic inputs. Organic Geochemistry 31(12), 1765-1781.
Peuravuori, J. and Pihlaja, K. (1997) Molecular size distribution and spectroscopic properties of aquatic humic substances. Anal.chim.acta 337(2), 133-149.
Razavi, M., Kompany-Zareh, M. and Khoshkam, M. (2021) PARAFAC study of L-cys@CdTe QDs interaction to BSA, cytochrome c and trypsin: An approach through electrostatic and covalent bonds. Spectrochimica Acta Part A: Molecular and Biomolecular Spectroscopy 246, 119016.
Sha, J., Lu, Z., Ye, J., Wang, G., Hu, Q., Chen, Y. and Zhang, X. (2019) The inhibition effect of recycled Scenedesmus acuminatus culture media: Influence of growth phase, inhibitor identification and removal. Algal Research 42, 101612.
Shang, Y., Song, K., Jacinthe, P.A., Wen, Z. and Liu, G. (2019a) Characterization of CDOM in reservoirs and its linkage to trophic status assessment across China using spectroscopic analysis. Journal of Hydrology 576, 1-11.
Shang, Y., Song, K., Jacinthe, P.A., Wen, Z., Lyu, L., Fang, C. and Liu, G. (2019b) Characterization of CDOM in reservoirs and its linkage to trophic status assessment across China using spectroscopic analysis. Journal of Hydrology 576, 1-11.
Shang, Y., Song, K., Wen, Z., Lyu, L., Zhao, Y., Fang, C. and Zhang, B. (2018) Characterization of CDOM absorption of reservoirs with its linkage of regions and ages across China. Environmental Science & Pollution Research 25(1993), 1-15.
Smith, V.H. (2003) Eutrophication of freshwater and coastal marine ecosystems a global problem. Environmental Science and Pollution Research 10(2), 126-139.
Smith, V.H. and Schindler, D.W. (2009) Eutrophication science: where do we go from here? Trends in Ecology & Evolution 24(4), 201-207.
Song, K., Li, L., Wang, Z., Liu, D., Zhang, B., Xu, J., Du, J., Li, L., Li, S. and Wang, Y. (2012) Retrieval of total suspended matter (TSM) and chlorophyll-a(Chl-a) concentration from remote-sensing data for drinking water resources. Environmental Monitoring & Assessment 184(3), 1449.
Song, K., Shang, Y., Wen, Z., Jacinthe, P.-A., Liu, G., Lyu, L. and Fang, C. (2019) Characterization of CDOM in saline and freshwater lakes across China using spectroscopic analysis. Water Research 150, 403-417.
Song, K., Wen, Z., Xu, Y., Yang, H., Lyu, L., Zhao, Y., Fang, C., Shang, Y. and Du, J. (2018) Dissolved carbon in a large variety of lakes across five limnetic regions in China. Journal of Hydrology 563, 143-154.
Stedmon, C.A. and Markager, S. (2005) Resolving the variability in dissolved organic matter fluorescence in a temperate estuary and its catchment using PARAFAC analysis. Limnology and Oceanography 50(2), 686-697.
Tang, X., Gao, G., Chao, J., Wang, X., Zhu, G. and Qin, B. (2010) Dynamics of organic-aggregate-associated bacterial communities and related environmental factors in Lake Taihu, a large eutrophic shallow lake in China. Limnology & Oceanography 55(2), 469-480.
Timko, S.A., Michael, G. and Cooper, W.J. (2015) Influence of pH on fluorescent dissolved organic

matter photo-degradation. Water Research 85, 266-274.
Traving, S.J., Mikkel, B.-T., Helle, K.-L., Mustafa, M., S., H.J.r.L., A., S.C., Helle, S.r., Stiig, M. and Lasse, R. Coupling Bacterioplankton Populations and Environment to Community Function in Coastal Temperate Waters. Frontiers in Microbiology 7.
Treseder, K.K. (2008) Nitrogen additions and microbial biomass: a meta-analysis of ecosystem studies. Ecology Letters 11(10), 1111-1120.
Vollenweider, R.A. (1968) Scientific Fundamentals of the Eutrophication of Lakes and Flowing Water, with Particular Reference to Nitrogen and Phosphorus as Factors in Eutrophication. Water Management Research 1970.
Wang, X., Wu, Y., Bao, H., Gan, S. and Zhang, J. (2019) Sources, Transport, and Transformation of Dissolved Organic Matter in a Large River System: Illustrated by the Changjiang River, China. Journal of Geophysical Research: Biogeosciences 124(12), 3881-3901.
Webster, K.E., Soranno, P.A., Cheruvelil, K.S., Bremigan, M.T., Downing, J.A., Vaux, P.D., Asplund, T.R., Bacon, L.C. and Connor, J. (2008) An empirical evaluation of the nutrient-color paradigm for lakes. Limnology and Oceanography 53(3), 1137-1148.
Wei, M., Gao, C., Zhou, Y., Duan, P. and Li, M. (2019) Variation in spectral characteristics of dissolved organic matter in inland rivers in various trophic states, and their relationship with phytoplankton. Ecological Indicators 104, 321-332.
Weishaar, J.L., Aiken, G.R., Bergamaschi, B.A., Fram, M.S., Fujii, R. and Mopper, K. (2003) Evaluation of Specific Ultraviolet Absorbance as an Indicator of the Chemical Composition and Reactivity of Dissolved Organic Carbon. Environmental Science & Technology 37(20), 4702-4708.
Wen, Z.D., Song, K.S., Zhao, Y., Du, J. and Ma, J.H. (2016) Influence of environmental factors on spectral characteristics of chromophoric dissolved organic matter (CDOM) in Inner Mongolia Plateau, China. Hydrology and Earth System Sciences 20(2), 787-801.
Wickland, K.P., Neff, J.C. and Aiken, G.R.J.E. (2007) Dissolved Organic Carbon in Alaskan Boreal Forest: Sources, Chemical Characteristics, and Biodegradability. 10(8), 1323-1340.
Williams, C.J., Frost, P.C., Morales-Williams, A.M., Larson, J.H., Richardson, W.B., Chiandet, A.S. and Xenopoulos, M.A. (2016) Human activities cause distinct dissolved organic matter composition across freshwater ecosystems. Global Change Biology 22(2), 613-626.
Wolfe, A.P., Kaushal, S.S., J Robin, F. and Mcknight, D.M. (2002) Spectrofluorescence of sediment humic substances and historical changes of lacustrine organic matter provenance in response to atmospheric nutrient enrichment. Environmental Science & Technology 36(15), 3217-3223.
Xiao, Y.H., Sara-Aho, T., Hartikainen, H. and Vähätalo, A.V. (2013) Contribution of ferric iron to light absorption by chromophoric dissolved organic matter. Limnology & Oceanography 58(2), 653-662.
Yao, X., Zhang, Y., Zhu, G., Qin, B., Feng, L., Cai, L. and Gao, G. (2011) Resolving the variability of CDOM fluorescence to differentiate the sources and fate of DOM in Lake Taihu and its tributaries. Chemosphere 82(2), 145-155.
Ye, L., Wu, X., Liu, B., Yan, D. and Kong, F. (2015) Dynamics and sources of dissolved organic carbon during phytoplankton bloom in hypereutrophic Lake Taihu (China). Limnologica 54, 5-13.
Zhang, X., Lu, Z., Wang, Y., Wensel, P., Sommerfeld, M. and Hu, Q. (2016) Recycling Nannochloropsis oceanica culture media and growth inhibitors characterization. Algal

Research 20, 282-290.
Zhang, Y., Qin, B., Zhang, L., Zhu, G. and Chen, W. (2005) Spectral Absorption and Fluorescence of Chromophoric Dissolved Organic Matter in Shallow Lakes in the Middle and Lower Reaches of the Yangtze River. Journal of Freshwater Ecology 20(3), 451-459.
Zhang, Y., Qin, B., Zhu, G., Zhang, L. and Yang, L. (2007) Chromophoric dissolved organic matter (CDOM) absorption characteristics in relation to fluorescence in Lake Taihu, China, a large shallow subtropical lake. Hydrobiologia 581(1), 43-52.
Zhang, Y., van Dijk, M.A., Liu, M., Zhu, G. and Qin, B. (2009) The contribution of phytoplankton degradation to chromophoric dissolved organic matter (CDOM) in eutrophic shallow lakes: Field and experimental evidence. Water Research 43(18), 4685-4697.
Zhang, Y., Zhang, E., Yin, Y., van Dijk, M.A., Feng, L., Shi, Z., Liu, M. and Qina, B. (2010) Characteristics and sources of chromophoric dissolved organic matter in lakes of the Yungui Plateau, China, differing in trophic state and altitude. Limnology and Oceanography 55(6), 2645-2659.
Zhang, Y., Zhou, Y., Shi, K., Qin, B., Yao, X. and Zhang, Y. (2018) Optical properties and composition changes in chromophoric dissolved organic matter along trophic gradients: Implications for monitoring and assessing lake eutrophication. Water Research 131, 255-263.
Zhao, H.C., Li, Y.P., Wang, S.R., Jiao, L.X. and Zhang, L. (2019) Fluorescence Characteristics of DOM in Overlying Water of Erhai Lake and Its Indication of Eutrophication. Spectroscopy and Spectral Analysis 39(12), 3888-3896.
Zhao, Y., Song, K., Li, S., Ma, J. and Wen, Z. (2016) Characterization of CDOM from urban waters in Northern-Northeastern China using excitation-emission matrix fluorescence and parallel factor analysis. Environmental Science and Pollution Research 23(15), 15381-15394.
Zhi, E., Yu, H., Duan, L., Han, L., Liu, L. and Song, Y. (2015) Characterization of the composition of water DOM in a surface flow constructed wetland using fluorescence spectroscopy coupled with derivative and PARAFAC. Environmental Earth Sciences 73(9), 5153-5161.
Zhou, Y.Q., Davidson, T.A., Yao, X.L., Zhang, Y.L., Jeppesen, E., de Souza, J.G., Wu, H.W., Shi, K. and Qin, B.Q. (2018) How autochthonous dissolved organic matter responds to eutrophication and climate warming: Evidence from a cross-continental data analysis and experiments. Earth-Science Reviews 185, 928-937.

# Figures

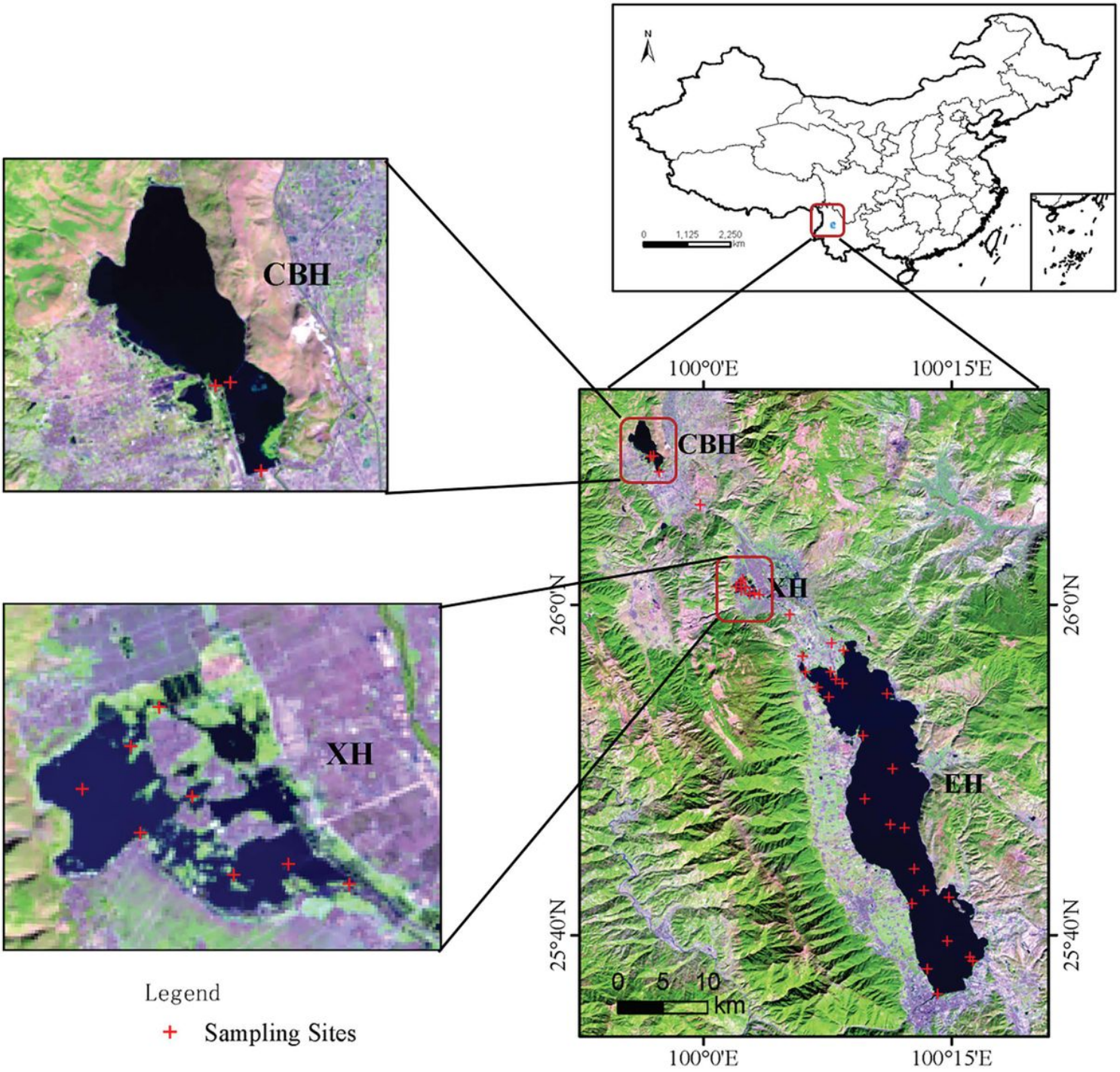


**Figure 1**

Sampling sites in the Erhai watershed, Yunan Province, China. EH: Lake Erhai, that located in Dali, Yunnan Province, China's seventh-largest freshwater lake; CBH: Lake Cibi, one of the upstream inflows of Lake Erhai as the major source; XH: Lake Xihu, the plateau freshwater lake located between EH and CBH. The red crosses represent the sampling sites

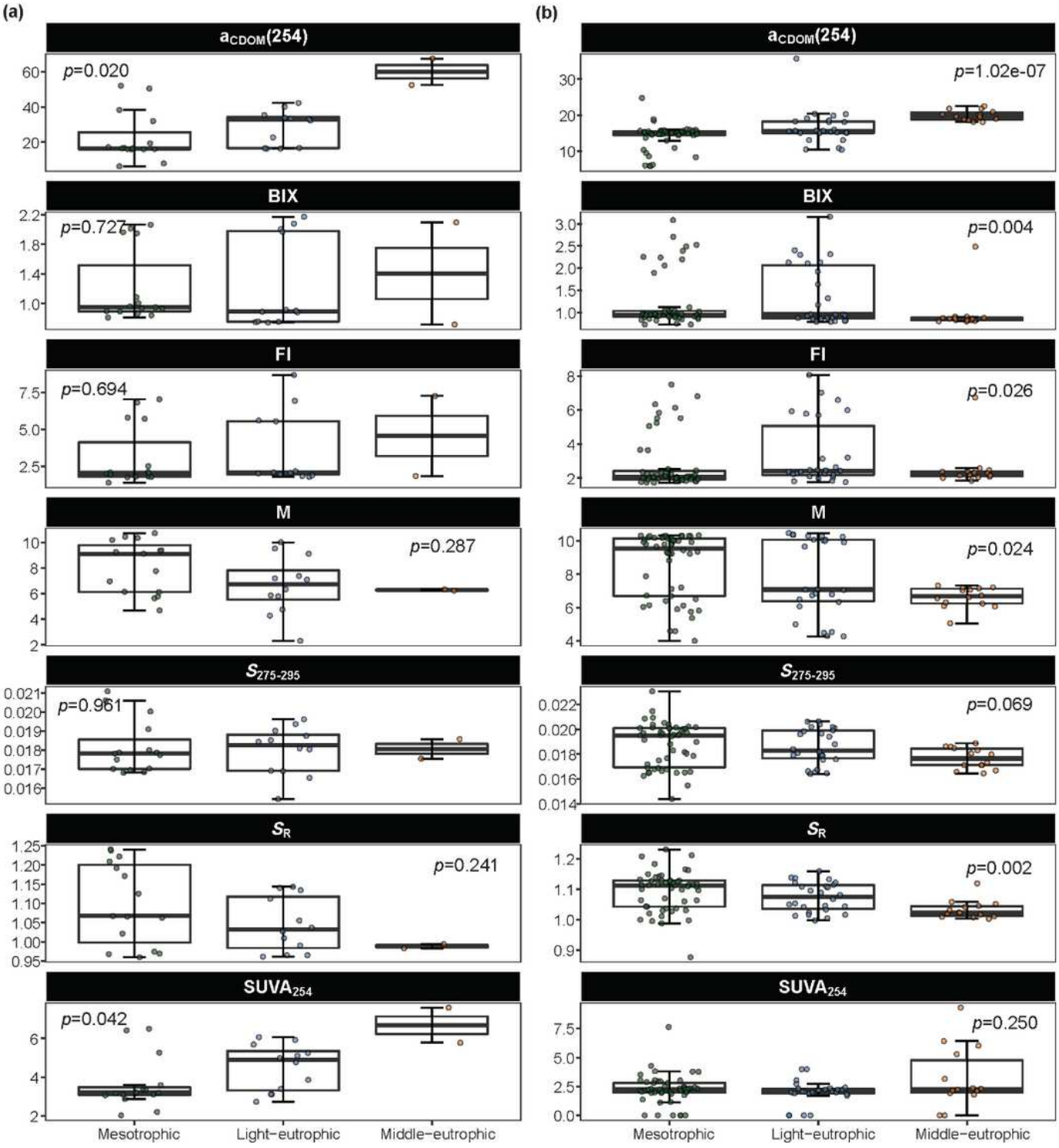


## Figure 2

The variation and comparison of aCDOM(254), BIX, FI, M, S275-295, SR and SUVA254 in different trophic states:(a) wet season; (b) dry season. The unit of aCDOM(254) was m-1, the unit of S275-295 was nm-1, and the unit of SUVA254 was L mg -1 m-1. p was based on K-W test. The line and circle within each box represent the median and values of samples, respectively. The color of the circle is on behalf of different trophic states.

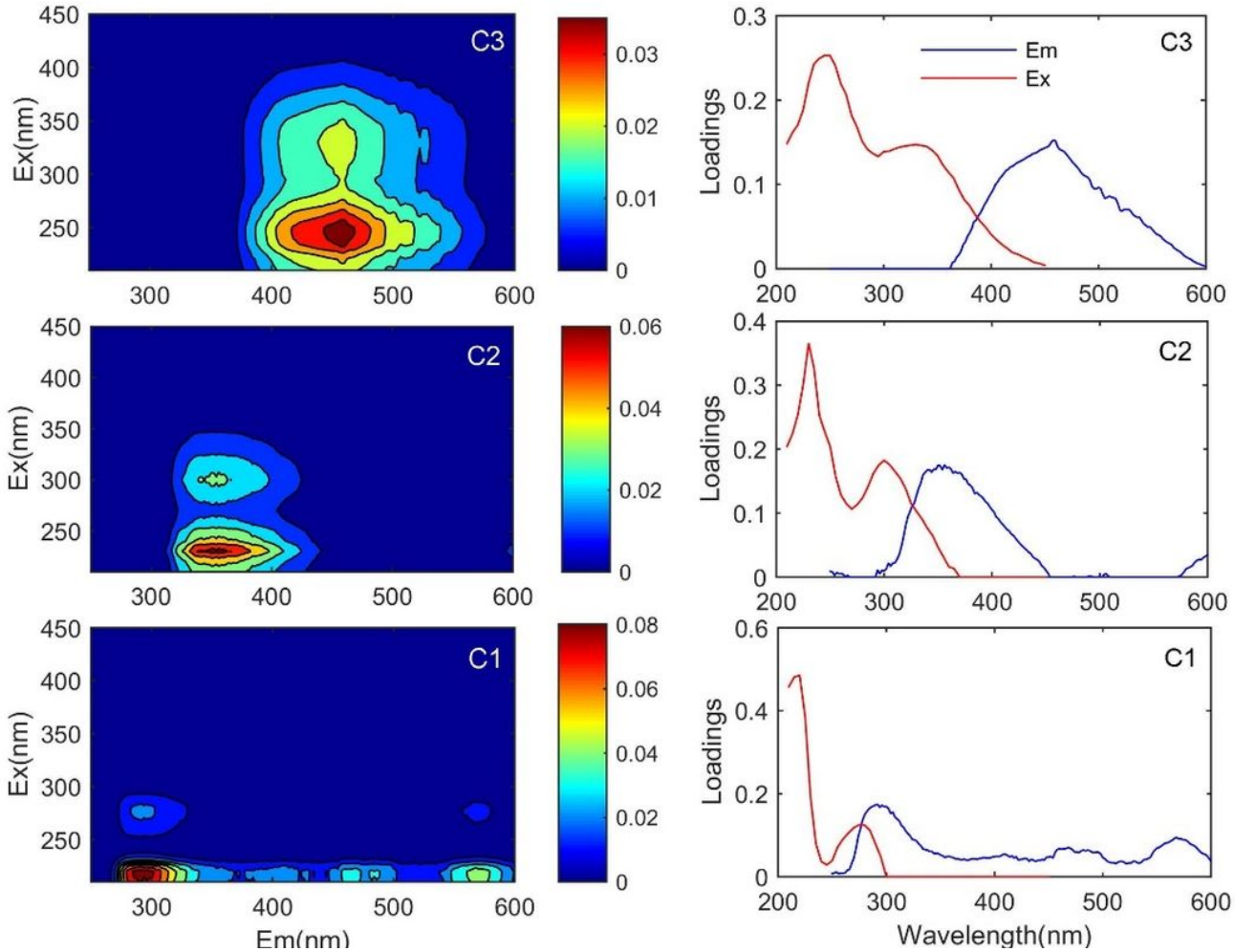


**Figure 3**

The output of parallel factor analysis (PARAFAC) referring to the fluorescent signatures of three components. Contour plots present the spectral shapes of excitation and emission. Line plots present split-half validation results of the corresponding component and show the excitation (red) and emission (blue) spectra of three unique split halves.

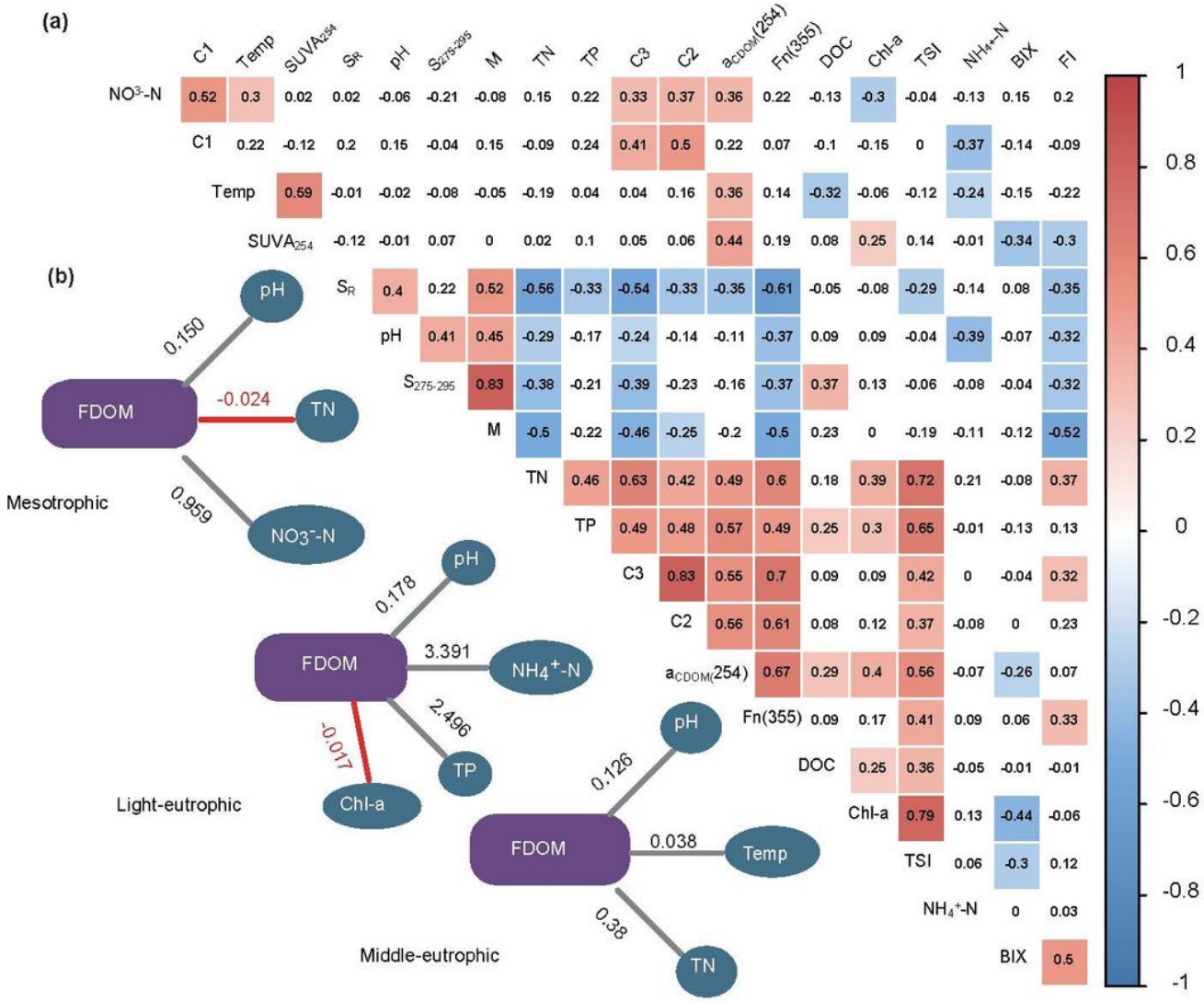


## Figure 4

(a) Spearman correlation analysis between water quality, the parameters of chromophoric dissolved organic matter (CDOM) and fluorescent dissolved organic matter (FDOM). Red and blue represent positive and negative correlations, respectively. The transparency of the square indicates the intensity of the correlation. The numbers within the table are the correlation coefficient. The blank background indicates p>0.01. (b) association network over correlation between environmental factors and FDOM by LASSO. Positive and negative correlation are shown as grey and red, and the number indicate coefficient.

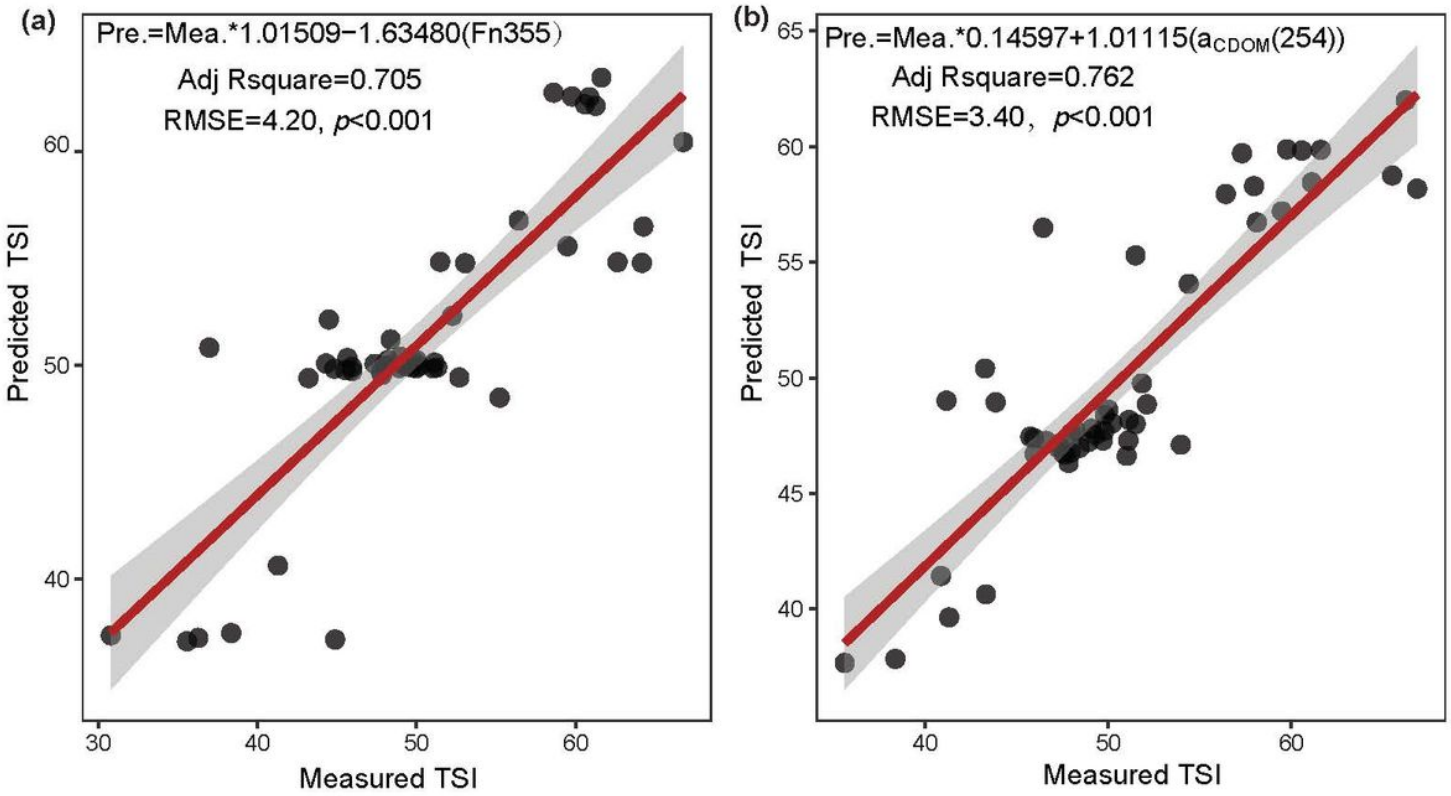


**Figure 5**

Validation results of TSI Model through comparison of measured TSI and predicted TSI in Erhai watershed. (a) predicted model based on aCDOM(254); (b) predicted model based on Fn(355). The red lines are trendlines with a confidence interval of 95%.

## Supplementary Files

This is a list of supplementary files associated with this preprint. Click to download.

- Graphicabstract.tiff
- Supplementary.docx